BMC Veterinary Research

RESEARCH

Open Access

Osteogenic potentials in canine mesenchymal stem cells: unraveling the efficacy of polycaprolactone/hydroxyapatite scaffolds in veterinary bone regeneration

Teeanutree Taephatthanasagon[1,2,3], Steven Dwi Purbantoro[2,3], Watchareewan Rodprasert[2,3], Koranis Pathanachai[2,3,4], Piyawan Charoenlertkul[2,3,4], Rangsini Mahanonda[6,7], Noppadol Sa-Ard-lam[6,7], Suryo Kuncorojakti[5], Adretta Soedarmanto[2,3], Nabila Syarifah Jamilah[2,3], Thanaphum Osathanon[8,9], Chenphop Sawangmake[2,3,4,9] and Sirirat Rattanapuchpong[2,3,10*]

Abstract

Background The integration of stem cells, signaling molecules, and biomaterial scaffolds is fundamental for the successful engineering of functional bone tissue. Currently, the development of composite scaffolds has emerged as an attractive approach to meet the criteria of ideal scaffolds utilized in bone tissue engineering (BTE) for facilitating bone regeneration in bone defects. Recently, the incorporation of polycaprolactone (PCL) with hydroxyapatite (HA) has been developed as one of the suitable substitutes for BTE applications owing to their promising osteogenic properties. In this study, a three-dimensional (3D) scaffold composed of PCL integrated with HA (PCL/HA) was prepared and assessed for its ability to support osteogenesis in vitro. Furthermore, this scaffold was evaluated explicitly for its efficacy in promoting the proliferation and osteogenic differentiation of canine bone marrow-derived mesenchymal stem cells (cBM-MSCs) to fill the knowledge gap regarding the use of composite scaffolds for BTE in the veterinary orthopedics field.

Results Our findings indicate that the PCL/HA scaffolds substantially supported the proliferation of cBM-MSCs. Notably, the group subjected to osteogenic induction exhibited a markedly upregulated expression of the osteogenic gene osterix (*OSX*) compared to the control group. Additionally, the construction of 3D scaffold constructs with differentiated cells and an extracellular matrix (ECM) was successfully imaged using scanning electron microscopy. Elemental analysis using a scanning electron microscope coupled with energy-dispersive X-ray spectroscopy confirmed that these constructs possessed the mineral content of bone-like compositions, particularly the presence of calcium and phosphorus.

Conclusions This research highlights the synergistic potential of PCL/HA scaffolds in concert with cBM-MSCs, presenting a multidisciplinary approach to scaffold fabrication that effectively regulates cell proliferation and

*Correspondence:
Sirirat Rattanapuchpong
sirirat.ra@chula.ac.th

Full list of author information is available at the end of the article

osteogenic differentiation. Future in vivo studies focusing on the repair and regeneration of bone defects are warranted to further explore the regenerative capacity of these constructs, with the ultimate goal of assessing their potential in veterinary clinical applications.

Keywords Canine bone marrow-derived mesenchymal stem cells (cBM-MSCs), Polycaprolactone/Hydroxyapatite (PCL/HA) scaffold, Bone tissue engineering, Bone regeneration, Veterinary, Osteogenic differentiation

Background

Surgical reconstruction of bone defects poses a significant challenge for the orthopedic surgeon. Such defects can arise from trauma, bone disorders, or the surgical resection of tumors and are often considered serious complications [1]. Presently, autogenous bone graft is the clinical gold standard [2]. However, this procedure faces limitations, including donor site morbidity and restricted availability of bone mass [3, 4]. To address these limitations, bone tissue engineering (BTE) has been extensively explored. BTE integrates three main components, which are osteogenic cell resources, biomaterials, and signaling molecules [5]. The aim of BTE is to enhance or replace biological tissues to repair bone defects. The ideal scaffold material for BTE should possess properties like osteoconductive, osteoinductive, biocompatible, biodegradable, and mechanical strength. Additionally, scaffold material should foster an environment conducive for stem cells to adhere, proliferate, and differentiate, thus regenerating new bone tissue in vivo [6, 7].

Recently, scaffolds with porous structures have been thoroughly examined for BTE, thanks to their ability to be constructed to mimic the microenvironment of natural bone architecture [8, 9]. Polycaprolactone (PCL), a synthetic polyester polymer, stands out as a widely investigated biomaterial for BTE. It offers desirable properties like adjustable porosity, biodegradability, and biocompatibility [10] and has Food and Drug Administration (FDA) approval for implantable applications [11, 12].

Hydroxyapatite (HA, $Ca_{10}(PO_4)_6(OH)_2$) is a bioactive ceramic closely resembling the inorganic component found in natural bone and teeth [13, 14]. Due to its biocompatibility, osteoconductivity, osteoinductivity, and hardness, HA is commonly used as a bioactive component of biomaterials in both orthopedics [15] and dentistry [16, 17]. Composite scaffolds, combining the strengths of various materials, have emerged as particularly promising in BTE [18]. While PCL offers several advantages, its unmodified form has poor cell attachment [19, 20] and mechanical properties [21, 22]. To address this, HA has been combined with PCL, resulting in enhanced mechanical attributes [23], osteogenic conduction [24], and osteogenic induction potential of the PCL/HA composite scaffolds [25].

Mesenchymal stem cells (MSCs) are multipotent and can differentiate into various cell lineages, including adipocyte, chondrocyte, and osteoblast [26]. Bone marrow-derived MSCs (BM-MSCs) have demonstrated promising osteogenic differentiation potential in humans [27] and animals [28]. Numerous studies have investigated the interplay between MSCs and scaffolds. For instance, research showed that PCL/HA composite scaffold supported the differentiation of human BM-MSCs into osteogenic lineage [29]. Similarly, rat BM-derived MSCs have also been shown to grow, proliferate, and differentiate towards osteogenic lineage in vitro when placed on PCL/HA scaffolds [30]. Yet, while there is significant data on human medical applications, research focusing on canine bone marrow-derived stem cells (cBM-MSCs) in veterinary clinical practice remains scarce.

In this regard, this study aims to explore the potential of PCL/HA scaffolds in facilitating the in vitro osteogenic differentiation of cBM-MSCs (Fig. 1). The findings could inform the development of translational strategies for the clinical application of canine stem cells and biomaterials for BTE in veterinary practice.

Results

Characterization of cBM-MSCs

The isolated cBM-MSCs presented the plastic-adherence, fibroblast-like morphology (Fig. 2A), and mRNA marker expression relating to stemness (*REX1* and *OCT4*) and proliferation (*KI67*) (Fig. 2B). Flow cytometry revealed expression of MSCs surface markers (CD73 and CD90) and minimal expression of hematopoietic surface marker (CD45) (Fig. 2C). cBM-MSCs differentiated into osteogenic, chondrogenic, and adipogenic lineages, evidenced by staining with Alizarin Red S, Alcian blue, and Oil red O, respectively (Fig. 2D-F). These findings could indicate that the isolated cBM-MSCs displayed characteristics consistent with MSCs.

Cytocompatibility of PCL/HA scaffolds

Microstructure examination of PCL/HA scaffolds and cells-scaffold constructs

PCL/HA scaffolds were successfully fabricated, and the microstructure of the materials was examined. SEM images revealed the distribution of porous structure (50X) with pore sizes ranging from 425 to 500 µm (300X and 1,500X) (Fig. 3A). This finding could indicate that all the inter-porous structures (salt particles) were successfully removed via the salt-leaching steps. The cells-seeded PCL/HA scaffolds maintained in normal culture

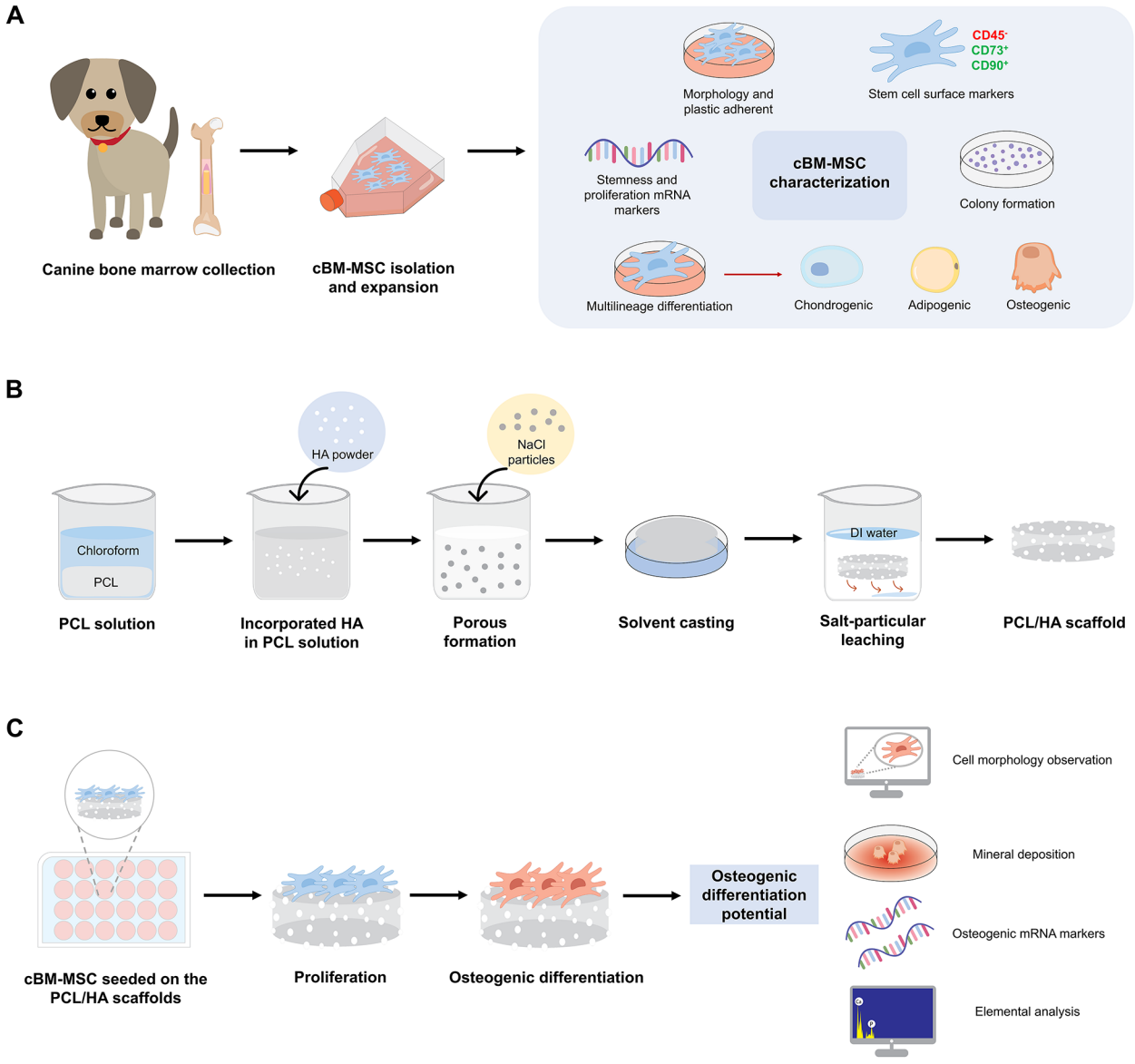

Fig. 1 A schematic illustration of the implementation of cBM-MSCs with fabricated PCL/HA scaffolds as BTE constructs. (**A**) The isolation and characterization of cBM-MSCs. (**B**) The preparation procedure of PCL/HA scaffold via solvent casting and salt particular leaching method. (**C**) The osteogenic differentiation of cBM-MSCs on PCL/HA scaffold and assessment of osteogenic potential of cell-seeded constructs

condition at 24 and 48 h post-seeded were investigated. cBM-MSCs adhered to both the surface and inner porous spaces of the scaffold (Fig. 3B). For 2D culture condition, the SEM images showed that the cBM-MSCs exhibited the fibroblast-like morphology, which rather similar to cells observed under phase-contrast microscope (Fig. 3C). Remarkably, cBM-MSCs cultivated in PCL/HA scaffolds possessed cell-to-cell contact in a 3D environment and retained fibroblast-like morphology in 3D culture (Fig. 3B). These results suggest that the PCL/HA scaffolds display favorable properties for providing a 3D environment with porous structures. This allows cBM-MSCs to access and adhere within the first 24 h. Subsequently, the cells continue to grow, expand, and engage in cell-to-cell interactions while maintaining cell viability up to 48 h after seeding.

In vitro cell proliferation analysis

The cell proliferation of cBM-MSCs under 2 different culture conditions was examined on day 1,5, and 7 post-seeding, as shown in Fig. 4A. In the 2D culture condition, there was a continuous increase in cell proliferation over time, with a significantly higher proliferation observed on day 7 compared to day 1 (Fig. 4B). When cBM-MSCs

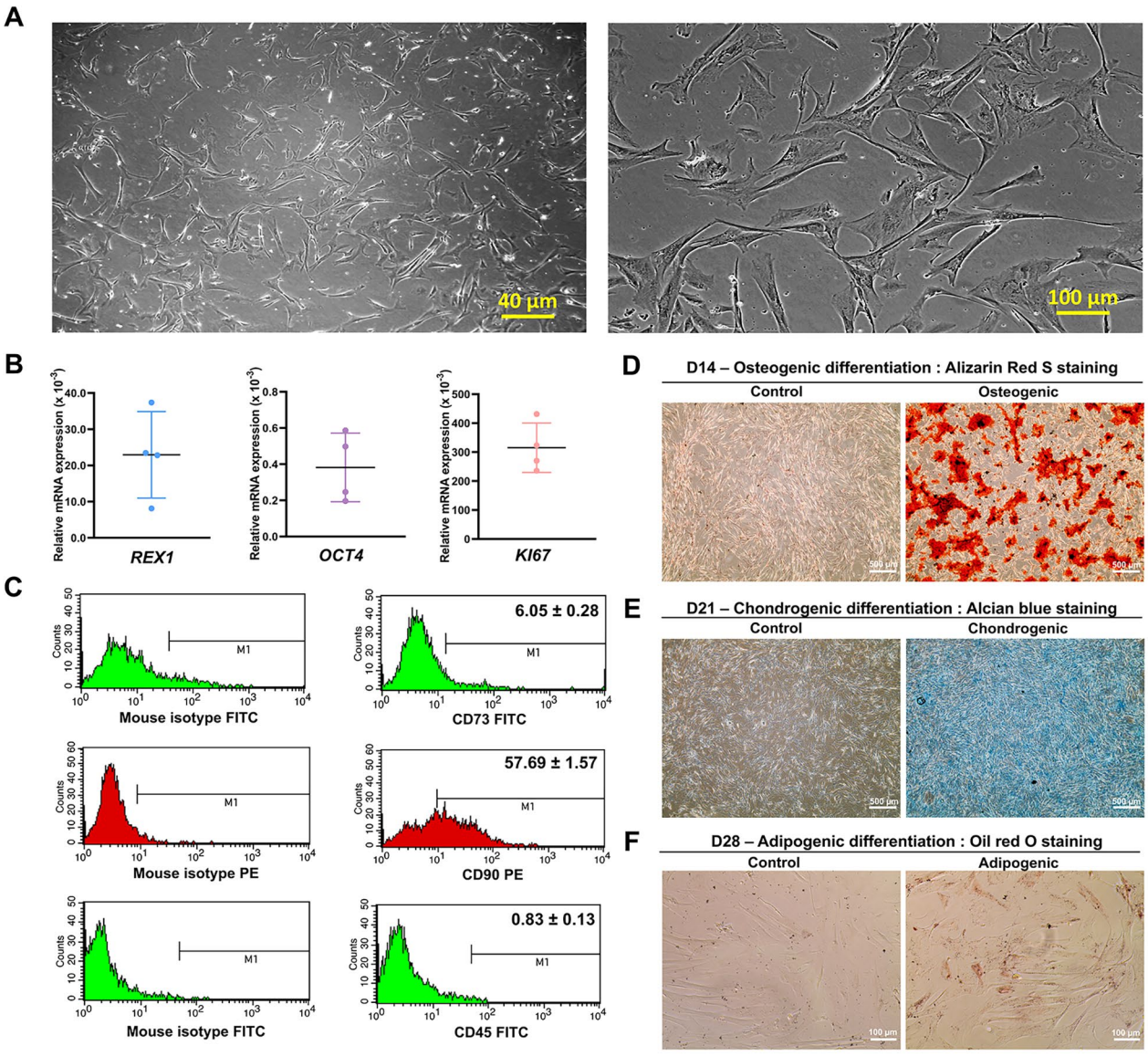

Fig. 2 Characterization of the isolated cBM-MSCs. (**A**) Morphology of cBM-MSCs. (**B**) RT-qPCR analysis of the expression of stemness (*REX1* and *OCT4*) and proliferation (*KI67*) marker of cBM-MSCs. (**C**) Flow cytometry analysis of the MSCs surface markers. (**D**) Alizarin red s, (**E**) Alcian blue, and (**F**) Oil red O staining for assessment of multilineage differentiation potential of cBM-MSCs through osteogenic, chodrogenic, and adipogenic lineage in vitro

were cultured on PCL/HA scaffolds in growth medium for 3 and 7 days, cell proliferation increased from day 1 to day 3 post-seeding, with the peak proliferation observed on day 3 post-seeding (Fig. 4C). These results demonstrated that the PCL/HA scaffolds developed in this study are biocompatible, allowing cBM-MSCs to grow and proliferate.

Effect of PCL/HA scaffolds on the osteogenic differentiation of cBM-MSCs in vitro

To access the osteogenic differentiation potential of cBM-MSCs using PCL/HA scaffolds, the cells were cultured on the scaffolds under osteogenic induction for 14 days, as depicted in Fig. 5A. After 14-day osteogenic induction, the matrix mineralization was examined using Alizarin Red S. The red staining from Alizarin was markedly evident in the osteogenically-induced group on the scaffolds compared to the undifferentiated control group (Fig. 5B). Additionally, quantification using Alizarin red elution revealed that the osteogenic induction group exhibited staining intensity approximately 10 times significantly higher than the undifferentiated control group (Fig. 5C). These findings suggested that cBM-MSCs can differentiate towards an osteogenic lineage on PCL/HA scaffolds in vitro while maintaining their mineral deposition ability.

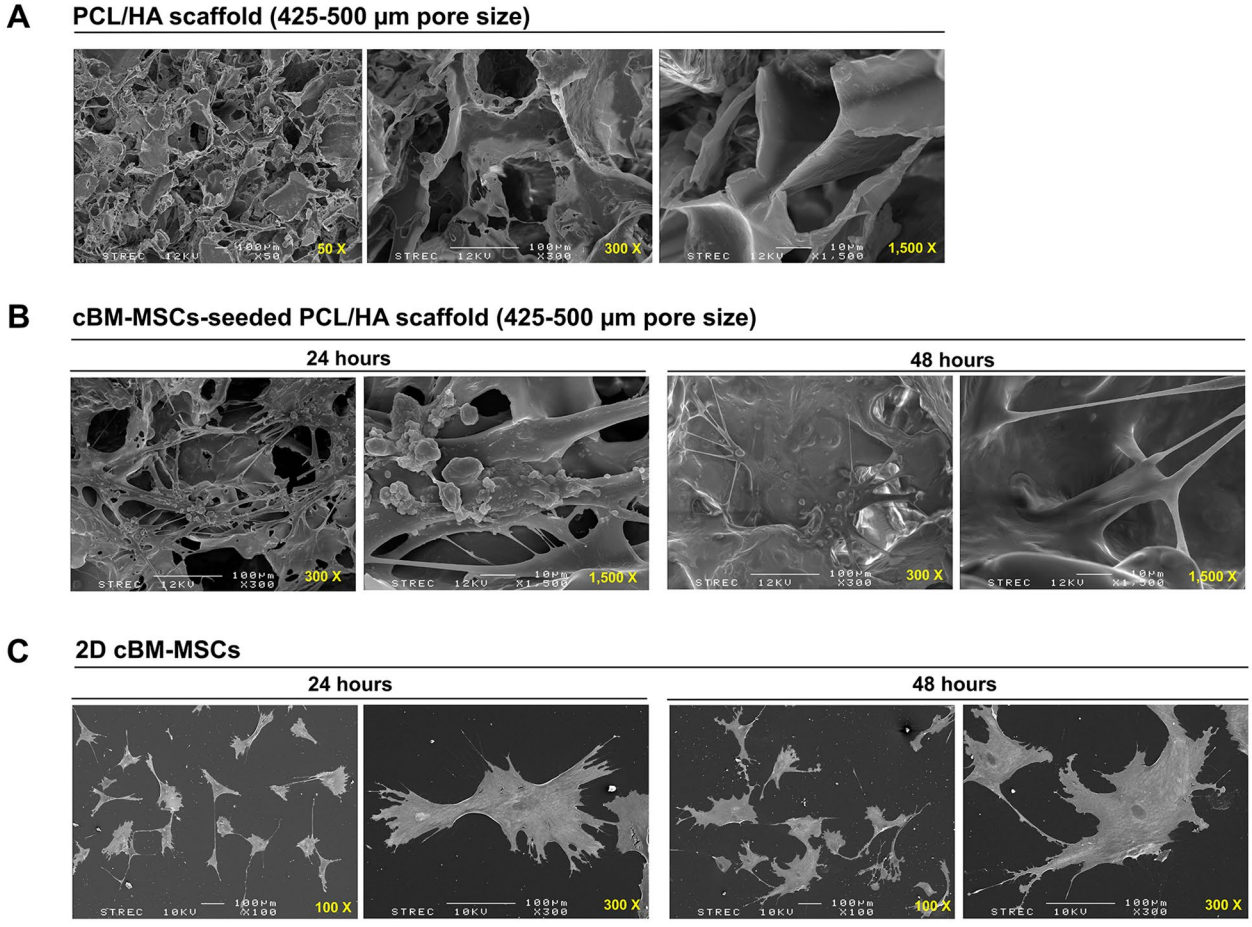

Fig. 3 Microstructure of PCL/HA scaffolds and cells-seeded scaffolds constructs. (**A**) SEM image at 50X, 300X, and 1,500X magnification illustrate the distribution of porous structure and pore size of fabricated PCL/HA scaffolds. SEM micrograph of the attachment of cBM-MSCs that were seeded in PCL/HA scaffolds (**B**) and were cultured in normal 2D culture condition (**C**) for 24 and 48 h

The expression of specific osteogenic-related mRNA is a key indicator of BM-MSCs differentiating toward an osteogenic lineage [31]. In this regard, the osteogenic mRNA expression levels of cBM-MSCs on PCL/HA scaffolds were analyzed on day 14 post-induction (Fig. 6A). The results from RT-qPCR revealed a significant upregulation of *OSX* in cBM-MSCs cultured with PCL/HA scaffolds in osteogenic induction environment. However, compared to the undifferentiated control group, the expression levels of the remaining osteogenic mRNA markers (*RUNX2*, *COL1A1*, *OCN*, *and OPN*) in the osteogenic group were not significantly different over the 14-day induction period (Fig. 6B).

To observe the microenvironment and mineralization of cells-seeded scaffolds after osteogenic induction, samples were evaluated using SEM/EDX on day 14 post-induction (Fig. 7A) Mineralized substances were exclusively found only in the osteogenic group (Fig. 7B). Consequently, the EDX analysis determined that the main elements in the mineralized regions of the PCL/HA scaffold, under osteogenic induction conditions, contained calcium and phosphorus (Fig. 7C). Combining the results from Alizarin Red S staining and elution, osteogenic mRNA expression from RT-qPCR, and SEM/EDX analysis, it can be indicated that the PCL/HA scaffold possesses the desired attributes to promote cBM-MSC growth, proliferation, and differentiation towards the osteogenic lineage, resulting in extracellular matrix mineralization in vitro.

Discussion

Bone tissue engineering has been proposed as a potential strategy for the repair and regeneration of maxillofacial bone defects in veterinary practice [32, 33]. This study explored the incorporation of two pivotal elements of BTE: stem cells and scaffolds. Regarding stem cell resources, cBM-MSCs have been reported as promising candidates for canine BTE. This is attributed to their ability to self-renew and multilineage differentiation [34, 35].

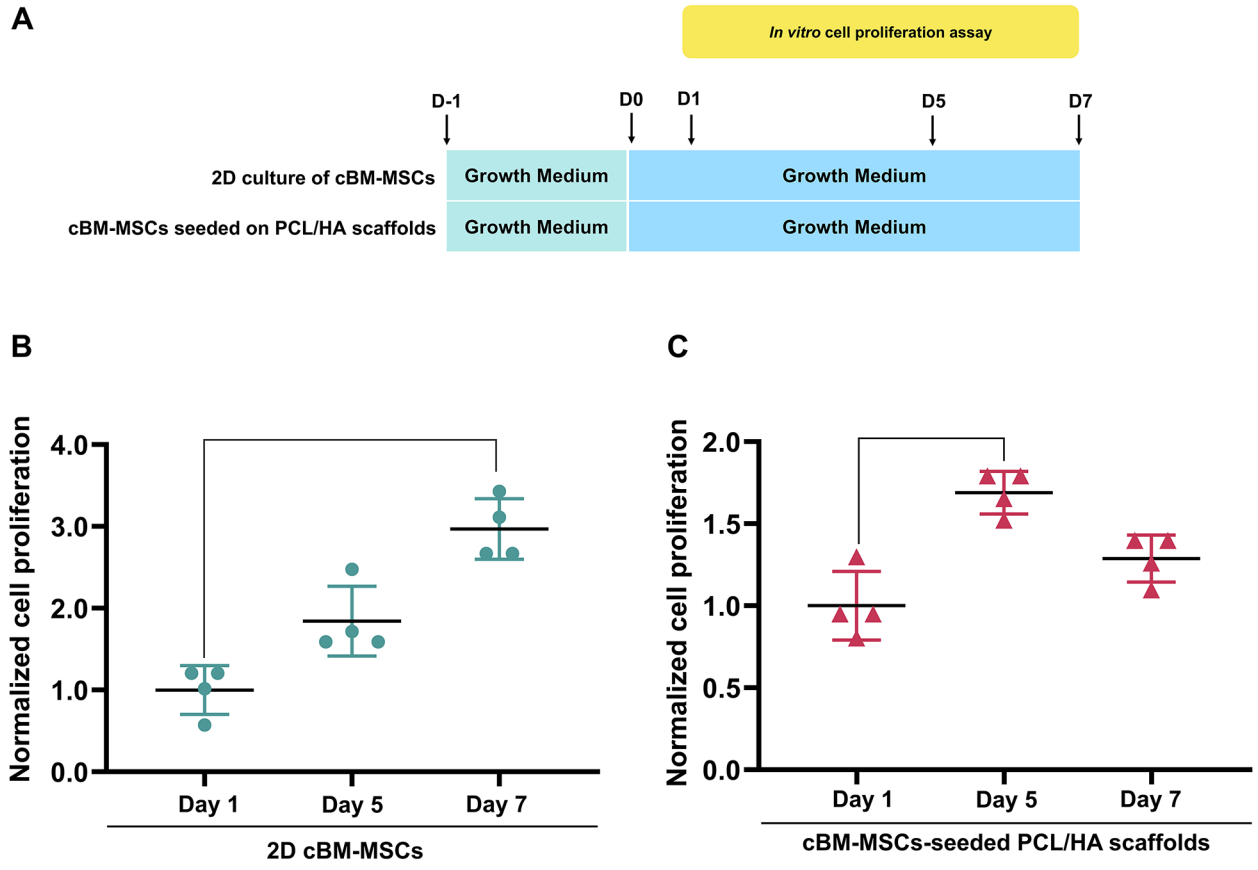

Fig. 4 Proliferation of cBM-MSCs cultured in vitro. (**A**) Schematic of experiment for cell proliferation. (**B**) Proliferation of cBM-MSCs under 2D condition and (**C**) on PCL/HA scaffolds which were explored at day 1,5, and 7 by MTT assay. Bars indicate the significant different compared to day 1 (p value < 0.05)

In this study, the isolated cBM-MSCs exhibited plastic adherence, specific cell surface marker expression, and multilineage differentiation capabilities, encompassing osteogenicity, chondrogenicity, and adipogenicity. These characteristics align with the criteria proposed by the International Society for Cellular Therapy (ISCT) [36]. While the expression of CD90 was moderately detected, the CD73 expression was relatively low. This level of CD73 expression aligns with findings from previous studies [37]. Notably, low CD73 expression has also been observed in canine MSCs from other tissue origins, including adipose tissues [38], dental pulp, and the periodontal ligament [39]. It has been established that the expression of specific surface markers in animal MSCs, such as CD73, CD90, and CD105, can vary by species and does not necessarily follow the trends observed in human MSCs [40]. Further research into the phenotypes of animal MSCs is warranted to gather comprehensive data on their characteristics. Beyond their stemness and specific surface marker expressions, which are prerequisites for MSC characterization, cBM-MSCs in this study demonstrated the ability to form mineralized nodules 14 days post-osteogenic induction and showed robust proliferation over a 7-day period under standard culture conditions. These findings underscore the potential of cBM-MSCs as promising stem cell candidates for BTE.

To realize bone tissue regeneration utilizing the BTE concept, the integration of key components, including potential stem cells and scaffolds, has been extensively investigated. In this study, the 3D PCL/HA scaffold was fabricated for cBM-MSCs culturing, aiming to emulate the three-dimensional in vivo environment, addressing one of the limitations of conventional 2D culture systems [41]. Additionally, the scaffold was designed with a porous architecture, given that the porous structure of biomaterials has been shown to significantly influence cell functions such as adhesion, migration, proliferation, and differentiation [42–44]. Consequently, we adopted the salt-particulate leaching method to generate this porous structure, owing to its benefits: the method allows for the creation of desired pore sizes based on the size of the porogens and is easy to process without the need for specialized equipment [7, 45]. As anticipated, the scaffolds obtained in this study exhibited an interconnected porous structure with a pore size ranging from

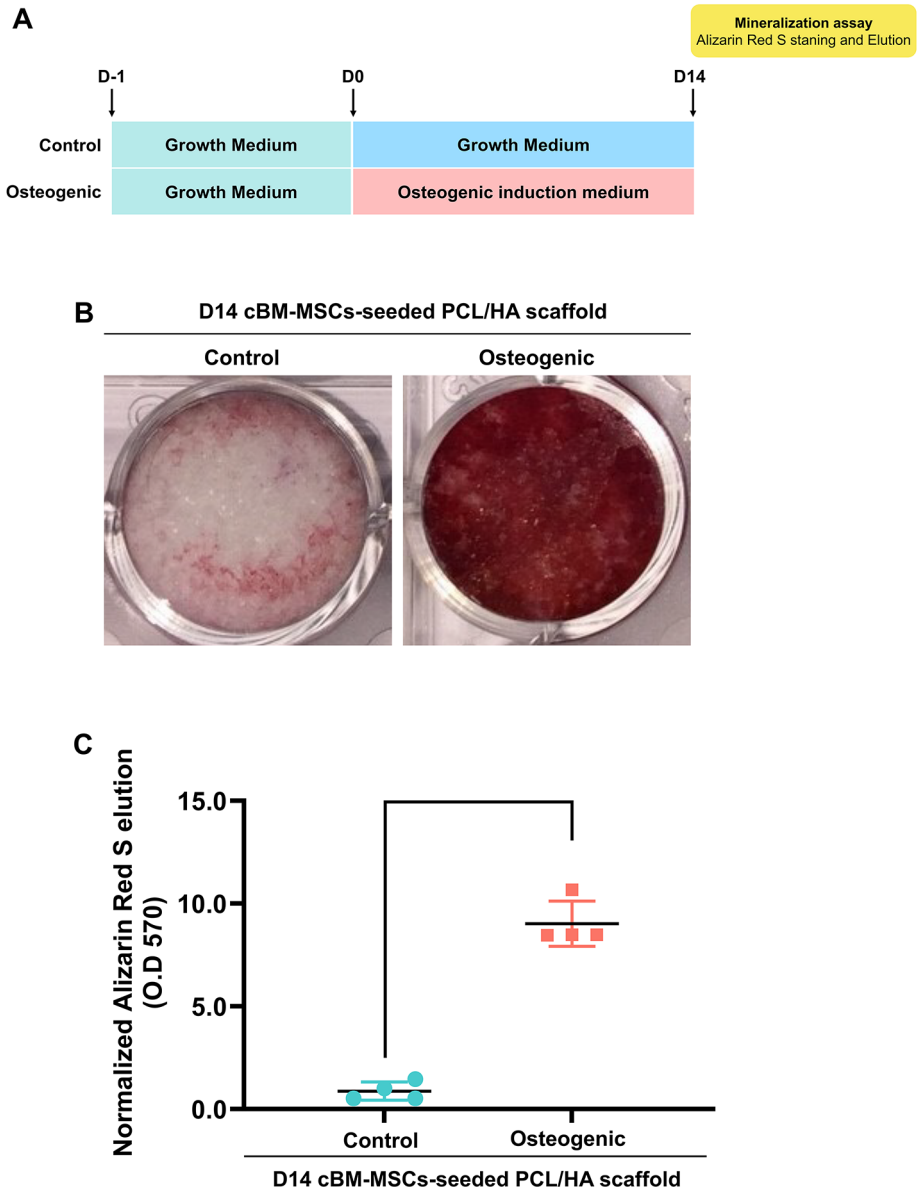

Fig. 5 Mineralization assay of cBM-MSCs-seeded PCL/HA constructs. (**A**) Schematic experiment of osteogenic induction of cBM-MSCs-seeded PCL/HA and the analyses of the mineral deposition. (**B**) Alizarin red S staining of cBM-MSCs-seeded PCL/HA scaffolds among undifferentiated control group and osteogenic induction group at day 14. (**C**) Quantitative analysis of Alizarin red staining between undifferentiated control group and osteogenic induction group at 14 days. Bars indicate the significant different between group (p value < 0.05)

425 to 500 μM with the sieved NaCl particles used in the salt-particulate leaching process.

A previous study constructed a porous PCL/HA-based scaffold with pore diameters ranging from 400 to 500 μM, showing that the fabricated scaffold enhanced the proliferation of MSCs derived from human bone marrow [29]. In this study, we examined the effect of the PCL/HA scaffold on cBM-MSCs proliferation, as there is limited in vitro data available on this topic. An increase in the O.D. value of formazan crystals from the MTT assay correlates with viable cells capable of converting the tetrazolium dye into a formazan product [46]. Based on the proliferation results, the PCL/HA scaffolds fabricated in this study were found to be biocompatible and had the desired properties to support the growth and proliferation of cBM-MSCs throughout the specified culture period. Moreover, cell numbers grew over the culture period, suggesting that the scaffolds promoted cell proliferation. While there was a slight decrease in cell proliferation on day 7, the difference between day 1 and

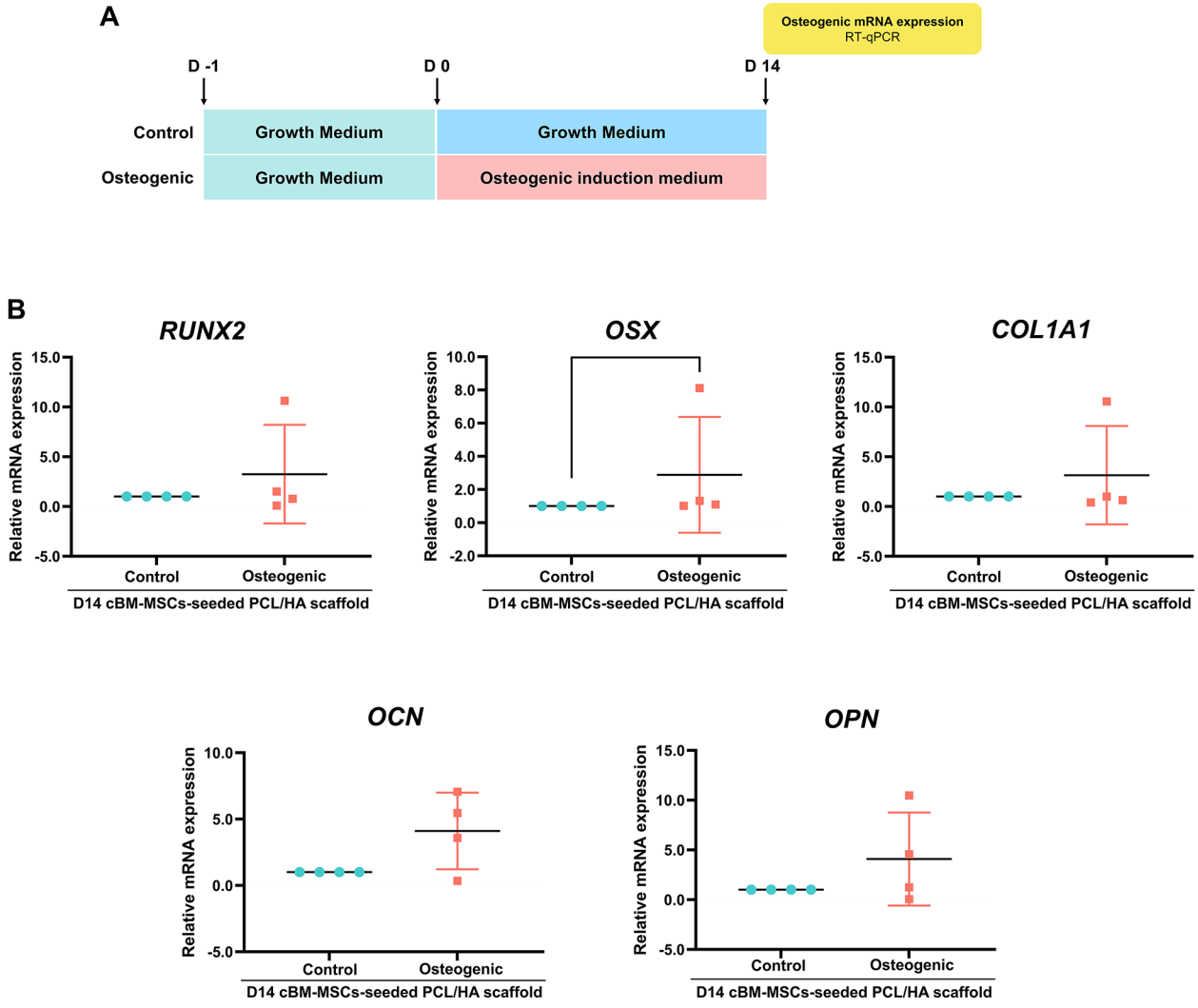

Fig. 6 RT-qPCR analysis of the osteogenic related marker expression of cBM-MSCs-seeded PCL/HA constructs. (**A**) Schematic diagram of an in vitro osteogenic induction and the evaluation of osteogenic mRNA markers. (**B**) Expression of osteogenic genes of *RUNX2*, *OSX*, *COL1A1*, *OCN*, and *OPN* after 14 days. Bars indicate the significant different between group (p value < 0.05)

day 7 post-seeding was not statistically significant. The observed pattern of cell proliferation, which shows an increase from day 1 to day 3 post-seeding followed by a slightly decrease at day 7 on PCL/HA scaffolds, can be attributed to several factors. The possible factors are the limited space for cell growth and oxygen depletion due to cell proliferation, which gradually occupies more surface area on the scaffold. Furthermore, the 3D structure of the PCL/HA scaffold may impose limitations on oxygen diffusion, particularly for cells located deeper within the scaffold. As cell density increases along the culture period, there is a demand for oxygen, which may result in hypoxic conditions that are unfavorable for continued cell proliferation [47].

The potential of PCL/HA scaffold to facilitate osteogenic differentiation of cBM-MSCs in vitro was investigated. Previous studies have shown that PCL/HA-based scaffolds can support the differentiation of BMSCs towards osteogenic lineage, both in human and animal models. In this study, we assessed the osteogenic differentiation of cBM-MSCs cultured on PCL/HA scaffolds. Positive Alizarin Red S staining on the cell-seeded PCL/HA scaffold indicates the ability of cBM-MSCs to differentiate towards an osteogenic lineage under osteogenic conditions. A similar result with Alizarin Red S was observed in a previous study, which examined the osteogenic differentiation of human BMSCs on micro-sized PCL/HA scaffolds. This previous research showed mineralization deposits after 28 days of osteogenic induction [48].

In addition to matrix mineralization, an upregulation of osteogenic-related mRNA markers was observed in

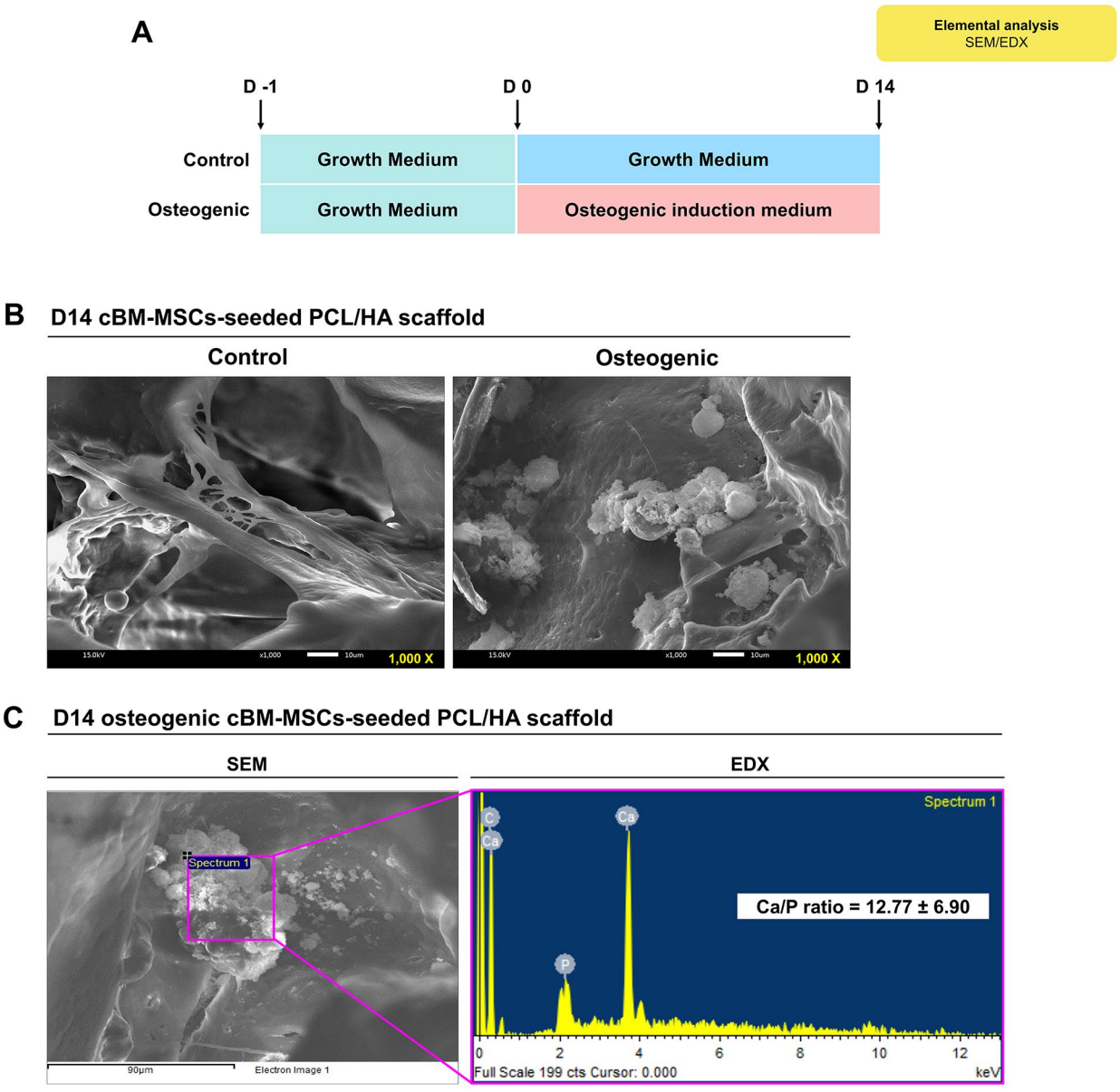

Fig. 7 Microarchitecture and mineralization assessment of cBM-MSCs-seeded PCL/HA scaffolds after osteogenic induction. (**A**) Schematic experiment of osteogenic induction of cBM-MSCs-seeded PCL/HA towards osteogenic lineage. (**B**) SEM image of cells-seeded PCL/HA among undifferentiated control group and osteogenic induction group at day 14. (**C**) EDX analysis of elements in mineralized nodule of cBM-MSCs-seeded PCL/HA constructs in osteogenic induction group. Data was calculated and presented as mean ± SD of calcium and phosphorus ratio

cBM-MSCs seeded on PCL/HA under osteogenic conditions. *RUNX2* is a pivotal transcription factor for guiding MSCs toward the osteogenic lineage in the early stage [49], while *OSX* functions as a transcription factor in the late stages of osteogenesis [50]. Our result demonstrated a significant upregulation of *OSX* in cBM-MSCs seeded on PCL/HA scaffolds under osteogenic conditions at day 14. This trend aligns with our previous findings from the osteogenic induction of cBM-MSCs in 2D culture conditions [28], suggesting the potential for cBM-MSCs to differentiate towards an osteogenic lineage on PCL/HA scaffolds within 14 days. Interestingly, the potential of PCL/HA-based scaffolds has also been observed in other species. A previous study conducted the osteogenic induction of rat MSCs using a PCL scaffold coated with HA and noted a marked upregulation of *OSX* by day 21 post-induction [30]. The differentiation of MSCs towards the osteogenic lineage is marked by the activation of *RUNX2*, an early transcription factor, and subsequently by *OSX* in the later stages. As differentiation progresses, *COL1A1* can be detected in early-stage osteoblasts [51], while *OCN* and *OPN* are evident in mature osteoblasts

[52]. Given this, the observed insignificant difference in the expression of *RUNX*2 and *COL1A1* between the two experimental groups in our study could be attributed to the mRNA being assessed on day 14. This timeframe is considered the final stage of cBM-MSC bone induction, which might lead to an indistinct variation in the expression of early-stage osteogenic mRNA markers. Additionally, we analyzed the mRNA expressions of *OCN* and *OPN*, which are associated with the process of matrix maturation and mineralization [53]. By day 14, the mRNA expressions of *OCN* were slightly upregulated in cBM-MSCs seeded on PCL/HA scaffolds under osteogenic induction when compared to the control group. However, the statistical significance was not noticed. This trend of non-significantly distinct upregulation of *OCN* during osteogenic induction was observed in a prior investigation with canine BM-MSCs in 2D culture systems in the presence of ECM, as evidenced by SEM [54]. Thus, it could be indicated that the PCL/HA scaffold might accelerate the differentiation of cBM-MSCs toward osteoblastic lineage, as *OCN* serves as a marker indicating mature osteoblasts. For the trend of *OPN* expression, a previous study demonstrated that OPN might hinder extracellular matrix mineralization by influencing mineral crystal formation [55]. This could explain the contentious outcomes of matrix mineralization which was accessed by ARS staining following osteogenic stimulation in our study. As a result, the limitation of the variety of primary cell cultures derived from distinct individuals, as well as the limited number of donor subjects, should be noted as one explanation that could affect the indistinct outcome of osteogenic mRNA expression.

The formation of mineral nodules was distinctly observed through SEM, and elemental analysis by EDX substantiated the accumulation of calcium and phosphorus in the cBM-MSCs-seeded on the PCL/HA scaffold under osteogenic media conditions. This accumulation was notably presented only in the osteogenic induction group, while it was not visible in the undifferentiated control group. Such findings infer the cellular deposition of new bone tissue, corroborated by ARS staining, which demonstrated distinct red spots indicative of mineralized areas in the ECM following a-14-day period of osteogenic induction. Notably, while the osteogenic differentiation potential of cBM-MSCs on PCL/HA scaffolds was evidenced in vitro, it is pertinent to highlight that cBM-MSCs in this study potentially required a shorter induction period for osteogenic differentiation. This variance might lead to a differential expression level of osteogenic markers during the induction phase on PCL/HA scaffolds, particularly when contrasted with MSCs derived from other species.

Conclusion

This investigation focused on evaluating the potential of the PCL/HA scaffold in facilitating the osteogenic differentiation of cBM-MSCs in an in vitro setting. The findings demonstrated that cBM-MSCs, differentiated on PCL/HA scaffolds, exhibit significant osteogenic potential, thereby highlighting their viability as a promising cell source for BTE. The in vitro experiments confirmed the biocompatibility of the PCL/HA scaffold, alongside its capacity to support stem cell growth, proliferation, and osteogenic differentiation, underlining its suitability for BTE applications. For a more comprehensive understanding, future research should endeavor to integrate these pivotal components with relevant signaling molecules in an in vivo context. This approach aims to explore the efficacy of these combined elements in repairing and regenerating bone defects, ultimately assessing their practical applicability and clinical feasibility in veterinary medicine.

Methods

Isolation, culture, and expansion of cBM-MSCs

The collection of cBM-MSCs was performed following the guidelines and regulations approved by the Institutional Animal Care and Use Committee (IACUC), Faculty of Veterinary Science, Chulalongkorn University (Animal Use Protocol No. 1531038). In this study, healthy dogs aged ranging from 3 to 10 years old were included as a criterion for bone marrow collection, with informed consent obtained from the pet owners. Bone marrow (BM) was collected according to the previously published protocol [56], with the procedure conducted by veterinarians at the Small Animal Teaching Hospital of Chulalongkorn University. Briefly, BM was aspirated from the iliac crest with an aseptic technique by using 18-gauge Jamshidi® bone marrow biopsy needles (BD, USA) with a 10 mL sterile syringe containing heparin solution in a ratio of 2,500 IU heparin to 1 mL bone marrow aspirate. The aspirated BM was then transported to the laboratory for processing to isolate the cBM-MSCs. Aspirated canine BM was washed twice with Hank's Balanced Salt Solution (HBSS, Thermo Fisher Scientific, USA). Consequently, the mixture was centrifuged at 300 g for 15 min and 1,000 g for 5 min, respectively. The supernatant was discarded, and the pellet was then gently resuspended and seeded onto T-75 culture flasks (Corning, USA).

cBM-MSCs were cultured in Dulbecco's Modified Eagle Medium/F12 (DMEM/F12) (Thermo Fisher Scientific, USA) supplemented with 10% fetal bovine serum (FBS) (Thermo Fisher Scientific, USA), 1% Glutamax (Thermo Fisher Scientific, USA), and 1% Antibiotic-Antimycotic (Thermo Fisher Scientific, USA). Then, cells were incubated at an appropriate environment of 5% CO2 with 95% air at 37 °C, and the culture medium was replaced

every 48 h. When cells reached 80% confluency, subculture was performed. Cells in passages 2 to 5 were used for all the following experiments.

Characterization of cBM-MSCs

The isolated cBM-MSCs were characterized for the characteristics of MSCs by observing the morphology of the cells under a phase-contrast microscope, the expression of mRNA markers relating to stemness (*REX1* and *OCT4*), and proliferation (*KI67*) by reverse transcription-quantitative polymerase chain reaction (RT-qPCR), the expression of cell surface markers related to MSCs by flow cytometry, and multilineage differentiation potential of cBM-MSCs. To characterize the expression of MSCs-related cell surface markers by flow cytometry, single-cell suspensions were stained with mouse anti-CD73 monoclonal antibody (Invitrogen, USA) and FITC-conjugated goat anti-mouse immunoglobulin G (IgG) secondary antibody (Bio-Rad, USA), PE-conjugated rat anti-CD90 monoclonal antibody (eBioscience, USA), and FITC-conjugated mouse anti-CD45 monoclonal antibody (Bio Legend, USA). For isotype control, mouse IgG2a kappa Isotype (BioLegend, USA), PE-conjugated rat IgG2b kappa Isotype (BioLegend, USA), and FITC-conjugated mouse IgG1 kappa Isotype (BioLegend, USA) were employed [28]. The assay was performed by using FACS-Calibur flow cytometer (BD bioscience, USA). ($n=3$)

To investigate the multilineage differentiation potential of cBM-MSCs, cBM-MSCs were inducted into 3 cell lineages, including osteogenic, chondrogenic, and adipogenic, following the protocol of a previously published study [28, 57].

In vitro osteogenic differentiation of cBM-MSCs was performed by seeding the cells onto the 24-well plate (Corning, USA) in the concentration of 35,000 cells/well and cultured in osteogenic induction medium which contains growth media and supplemented including 50 µg/mL ascorbic acid (Sigma-Aldrich, USA), 100 nM dexamethasone (Sigma-Aldrich, USA), and 10 mM β-glycerophosphate (Sigma-Aldrich, USA) for 14 days. Osteogenic differentiation was verified by using Alizarin Red S to detect the mineralization in the extracellular matrix after 14 days post-induction.

For in vitro chondrogenic differentiation, cells were seeded onto the 24-well plate in concentration of 50,000 cells/well and cultured in a chondrogenic induction medium which contained 15% FBS in growth media and supplemented including 0.1 µM dexamethasone (Sigma-Aldrich, USA), 50 µg/mL L-ascorbic-2-2phosphate (Sigma-Aldrich, USA), 40 mg/mL L-proline (Sigma-Aldrich, USA), 1% of insulin-transferrin-selenium (ITS, Thermo Fisher Scientific, USA) and 10 ng/mL of transforming growth factor-β3 (TGF-β3) (Sigma-Aldrich, USA), and 2% Antibiotic–Antimycotic supplement for 21 days. Cells were stained with Alcian blue (Sigma-Aldrich, USA) after 21 days of chondrogenic induction to detect the glycosaminoglycan.

For in vitro adipogenic differentiation, cBM-MSCs in concentration of 30,000 cells/well were seeded onto a 24-well plate and cultured in adipogenic induction medium supplemented with 0.1 mg/mL insulin (Sigma-Aldrich, USA), 1 µM dexamethasone (Sigma-Aldrich, USA), 1 mM of 3-isobutyl-1-methylxanthine (IBMX) (Sigma-Aldrich, USA), 0.2 mM indomethacin (Sigma-Aldrich, USA) for 28 days. Subsequently, cells were then stained with Oil red O (Sigma-Aldrich, USA) to detect the intracellular lipid droplets.

Fabrication of polycaprolactone (PCL) incorporated with hydroxyapatite (HA) or PCL/HA scaffolds and microarchitecture observation

To fabricate the PCL/HA scaffolds, solvent-casting and salt particulate-leaching techniques modified from previous published studies [29, 58] were used in this study. For the steps of solvent-casting, 28% w/v PCL solution was prepared by dissolving PCL pellets (80,000 MW; Sigma-Aldrich, UK) in chloroform (Sigma-Aldrich, USA) at room temperature and continuously stirring for 2 h. Consequently, commercial HA powder (Sigma-Aldrich, USA) of approximately 40% w/w of PCL was added and mixed with the PCL solution. To create the porous of PCL/HA scaffolds, NaCl particles were used as a porogen in this study. Before being mixed with PCL/HA solution, NaCl particles (Sigma-Aldrich, USA) were sieved to obtain the particle diameters of 425 to 500 µm in range and were then added into the PCL/HA solution in the ratio 1:10 of PCL: NaCl. Subsequently, the mixture was packed into the glass Petri dishes with a thickness of 5 mm to form the thin-cylindrical shape of PCL/HA scaffolds. After that, the PCL/HA molds were placed in a fume hood for 48 h to let the solvent evaporate from the scaffolds. For the steps of salt particulate-leaching, the dried-prepared PCL/HA scaffolds were immersed in deionized water with the continuous stirring for 48 h to let the NaCl particles leached out into the water and the scaffolds possessed the porous structure. The water was changed every 4 h to discard the leached-out NaCl particles. Then, PCL/HA scaffolds were air-dried overnight and punched to create the cylindrical shape of the scaffold by a 16-mm-diameter biopsy punch. Subsequently, the surface morphology and microstructure of the fabricated PCL/HA scaffolds were evaluated by using a Scanning electron microscope (SEM) (JEOL JSM-IT300).

cBM-MSCs cultured onto PCL/HA scaffolds

To examine the cytocompatibility of fabricated PCL/HA scaffolds, culturing of cBM-MSCs on the scaffolds was performed. Briefly, the PCL/HA scaffolds were made

into small discs by using a biopsy punch. The PCL/HA scaffolds were then sterilized by plasma sterilization. Additionally, PCL/HA scaffolds were disinfected by immersed in 70% ethanol for 30 min and subsequently exposed to UV light for 30 min each side before rinsed with sterilized phosphate buffer saline (PBS) and normal DMEM. The PCL/HA scaffolds were placed into a 24-well plate (Corning, USA) containing DMEM/F12 (Thermo Fisher Scientific, USA) supplemented with 10% fetal bovine serum (FBS) (Thermo Fisher Scientific, USA), 1% Glutamax (Thermo Fisher Scientific, USA), and 1% Antibiotic-Antimycotic (Thermo Fisher Scientific, USA). cBM-MSCs with 80% confluency were trypsinized and directly seeded onto each scaffold at the density of 300,000 cells per scaffold. Consequently, the cell-seeded scaffolds were incubated in 5% CO_2 with 95% air at 37 °C, and the culture medium was replaced every 48 h until the following analyses. For the 2D culture condition, cBM-MSCs were seeded onto a 24-well plate (Corning, USA) at a density of 10,000 cells per well and were then cultured in the similar culture media as described above. Cells were incubated at 37 °C in 5% CO_2 with 95% air, and culture medium was replaced every 48 h until the following analyses.

Microstructure examination of cells-seeded PCL/HA scaffolds

To observe the cell morphology in the porous PCL/HA scaffolds, cBM-MSCs were seeded in a 24-well plate with previously placed PCL/HA scaffolds at a density of 300,000 cells per scaffold. Subsequently, SEM was employed to examine the microstructure of cell-scaffold constructs at 24 and 48 h post-seeded. Furthermore, normal-cultured 2D cells were also analyzed using an SEM.

In vitro cell proliferation assay

The cell proliferation of cBM-MSCs cultured in both PCL/HA scaffolds and 24-well plates was determined at different time points by using the 3-(4,5-dimethylthiazol-2-yl)-2,5-diphenyltetrazolium bromide (MTT) assay according to the manufacturer's protocol. cBM-MSCs were cultured as described in 2.4. After 1,5 and 7 days post-seeding, the old medium was discarded before gently washing the cells with 500 µL of pre-warmed sterile PBS per well. 300 µL of MTT working solution (0.5 mg/mL) was added to each well, and the cells were incubated in 5% CO_2 with 95% air at 37 °C for 20 min. To dissolve the formazan crystal in the elution steps, the MTT solution was discarded, followed by adding 1 mL of elution buffer, which contained glycine buffered-dimethyl sulfoxide (DMSO), into each well. Then, optical density or O.D. was measured at wavelengths of 570 nm by using a spectrophotometer. The results obtained on each day were normalized to day 1 of each group and presented as normalized cell proliferation. ($n=4$)

In vitro osteogenic differentiation study

To explore the osteogenic differentiation of cBM-MSCs on PCL/HA scaffolds in vitro, the osteogenic differentiation was performed following our previous published studies [28, 56]. Firstly, pre-sterilized PCL/HA scaffolds ($n=4$) for each group were placed into a 24-well plate after being pre-washed with normal DMEM. The cells were then directly seeded onto each scaffold at a density of 300,000 cells per scaffold and cultured in an osteogenic induction medium with a similar composition as described in 2.2 for 14 days. Consequently, the cell-seeded scaffolds were incubated in 5% CO2 with 95% air at 37 °C, and osteogenic induction medium was routinely substituted every 48 h. Cells cultured on PCL/HA scaffolds supplemented with normal growth medium were used as the undifferentiated control group. To determine the effect of PCL/HA scaffolds on the osteogenic differentiation potential of cBM-MSCs, cells-seeded scaffolds were then further analyzed by performing the following methods, including mineralization assay, osteogenic-related mRNA markers evaluation, and elemental composition analysis after 14 days of osteogenic differentiation. ($n=4$)

Mineralization assay

To detect the mineralization in the extracellular matrix (ECM) of cells-seeded scaffolds, Alizarin red S (ARS) staining and elution were utilized in this study according to the previously published protocol [59]. Briefly, after 14 days of osteogenic induction, cells-seeded scaffolds were gently washed with PBS and fixed with cold methanol at 4 °C for 20 min. Then, the samples were washed with distilled water 3 times before being stained with a 2% ARS solution pH 4.2 (Sigma-Aldrich, USA) for 5 min at room temperature. The stained samples were then washed with distilled water (pH 4.2) for 3 times. Images of red-stained ECM mineralized nodules on cell-seeded scaffolds were captured. To quantitate the amount of stained ARS in the cell-scaffold constructs, the elution step was performed by adding 10% cetylpyridinium chloride (CPC) as an eluting solution into each well. Subsequently, in this study, O.D. was measured at wavelengths of 570 nm [29] by using a spectrophotometer. ($n=4$)

Reverse transcription-quantitative polymerase chain reaction (RTqPCR)

To access the expression of mRNA markers related to stemness (*REX1* and *OCT4*), proliferation (*KI67*), and osteogenic differentiation (*RUNX2*, *OSX*, *COL1A1*, *OCN*, and *OPN*), RT-qPCR was used in this study. TRIzol® reagent (Thermo Fisher Scientific, USA) and Direct-Zol

Table 1 Primer sequences of target genes using for RT-qPCR

Gene	Accession number	Sequences	(5′-3′)	Length (bp)	Tm (°C)
Stemness genes					
zinc finger protein 42 (*ZFP42 or REX1*)	XM_003639567.1	Forward	AGGTTCTCACAGCAAGCTCA	199	59.24
		Reverse	CCAGCAAATTCTGCGCACTG		60.73
octamer-binding transcription factor 4 (*OCT4*)	XM_538830.1	Forward	AGGAGAAGCTGGAGCAAAACC	100	60.55
		Reverse	GTGATCCTCTTCTGCTTCAGGA		59.50
Proliferation marker					
proliferation marker protein Ki-67 (*KI67*)	XM_014108788.1	Forward	GTGCAACTAAAGCACGGAGA	124	58.49
		Reverse	GAGATTCCTGTTTGCGTTTTCGT		58.49
Osteogenic markers					
runt-related transcription factor 2 (*RUNX2*)	XM_005642335.1	Forward	GGAAGAGGCAAGAGTTTCACC	209	58.84
		Reverse	GTGCTCACTTGCCAACAGAA		58.89
osterix (*OSX*)	XM_844688.3	Forward	GCGTCCTCCCTGCTTGAG	122	60.13
		Reverse	GCTTTGCCCAGTGTCGTTG		60.01
collagen type I alpha 1 chain (*COL1A1*)	NM_001003090.1	Forward	CCAGCCGCAAAGAGTCTACAT	150	60.41
		Reverse	CTGTACGCAGGTGACTGGTG		60.67
osteocalcin (*OCN*)	XM_547536.4	Forward	GCCAGCCTATGGTCTCCTCTG	249	61.90
		Reverse	CCACCAGCTCCTTCTGTTCTCT		54.55
osteopontin (*OPN*)	XM_003434024.2	Forward	GCCACAGAGCAAGGAAAACTC	180	59.73
		Reverse	CTGCTTCTGAGATGGGTCAGG		60.13
Reference gene					
glyceraldehyde 3-phosphate dehydrogenase (*GAPDH*)	NM_001003142.1	Forward	CCAACTGCTTGGCTCCTCTA	100	59.38
		Reverse	GTCTTCTGGGTGGCAGTGAT		59.67

RNA isolation kit (ZymoResearch, USA) were used to collect the total RNA of the cells following the manufacturer's protocol. RNA was then converted into complementary DNA (cDNA) by using Improm-II™ Reverse Transcription System kit (Promega, USA). Quantitative real-time PCR (qPCR) was performed with PowerUp™ SYBR™ Green Master Mix (Thermo Fisher Scientific, USA) using a Bio-Rad Real-Time PCR Detection System. Primers used in this study were summarized in Table 1. To normalize targeted mRNA expression, glyceraldehyde 3-phosphate dehydrogenase (*GAPDH*) gene was used as the reference gene. The mRNA expression was presented as a relative mRNA expression by normalizing it to *GAPDH* and control. The primer sequences are listed in Table 1.

Scanning electron microscope equipped with an energy-dispersive X-ray spectrometer (SEM/EDX) analysis

To evaluate the elemental components of cells-secreted and mineralized in the scaffolds, SEM (JEOL JSM-IT300) coupled with energy dispersive X-ray spectrometer (EDS: X-Max 20, Oxford) was employed in this study. After 14 days of osteogenic differentiation, cells-seeded scaffolds in both osteogenic and undifferentiated control group were examined by SEM/EDX analysis to study the microstructure of cells-seeded scaffolds and evaluate the elemental compositions in ECM constructs. The calcium and phosphorus ratio was evaluated from different biological samples and calculated using the percent weight of each element. Data was presented as mean ± standard deviation (SD). ($n=3$)

Statistical analysis

The results were presented as a dot plot ($n=4$) using GraphPad Prism 9.0 (Graph Software Inc., San Diego, CA). All data were analyzed by using SPSS software version 28.0 (IBM Corporation, USA) and presented as mean ± SD. The difference between the two independent groups was analyzed by the Mann-Whitney U test, while the Kruskal-Wallis test was employed for analyzing the comparison, which has more than two groups. Statistical difference was considered as significant when p value < 0.05.

Abbreviations

3D	Three-dimensional
ARS	Alizarin red S
BM	Bone marrow
BTE	Bone tissue engineering
cBM-MSCs	Canine bone marrow-derived mesenchymal stem cells
ECM	Extracellular matrix
FDA	Food and Drug Administration
HA	Hydroxyapatite
IACUC	Institutional Animal Care and Use Committee
ISCT	International Society for Cellular Therapy
MSCs	Mesenchymal stem cells
MTT	3-(4,5-dimethylthiazol-2-yl)-2,5-diphenyltetrazolium bromide
PCL/HA	Polycaprolactone/Hydroxyapatite
PCL	Polycaprolactone
RT-qPCR	Reverse transcription quantitative polymerase chain reaction
SEM/EDX	Scanning Electron Microscope equipped with an energy dispersive X-ray Spectrometer
SEM	Scanning electron microscope

Acknowledgements
The first author would like to thank The Second Century Fund (C2F), Chulalongkorn University for supporting the educational tuition fees and monthly expenses.

Author contributions
TT: data curation, formal analysis, methodology, investigation, visualization, writing – original draft, and writing – review & editing. SDP: formal analysis, methodology, investigation, writing – original draft, and writing – review & editing. WR: formal analysis, conceptualization, and writing – review & editing. KP and PC: data curation, methodology, investigation, and resources. RM and NS: investigation and resources. SK, AS, and NSJ: formal analysis, investigation, and writing – original draft. TO: conceptualization, resources, and supervision. CS: conceptualization, resources, supervision, validation, funding acquisition, and writing – review & editing. SR: conceptualization, funding acquisition, project administration, validation, and writing – review & editing. All authors reviewed and approved the final manuscript.

Funding
TT and SDP were supported by The Second Century Fund (C2F), Chulalongkorn University for Doctoral Scholarship. CS was supported by the Research Supporting Grant, Faculty of Veterinary Science, Chulalongkorn University; the Ratchadaphiseksomphot Endowment Fund, Chulalongkorn University; the Veterinary Clinical Stem Cell and Bioengineering Research Unit, Chulalongkorn University; and the Thailand Science Research and Innovation Fund Chulalongkorn University. SR was supported by the Grants for Development of New Faculty Staff, Ratchadaphiseksomphot Endowment Fund, Chulalongkorn University; Thailand Science research and Innovation Fund Chulalongkorn University; and the Research Grant, Faculty of Veterinary Science, Chulalongkorn University.

Data availability
The datasets used and/or analysed during the current study are available from the corresponding author on reasonable request.

Declarations

Ethics approval and consent to participate
The study involving canine bone marrow tissue collection was approved by the Institutional Animal Care and Use Committee (IACUC), Faculty of Veterinary Science, Chulalongkorn University (Animal Use Protocol No. 1531038). Bone marrow collection was conducted with informed consent obtained from the pet owners for the inclusion of their pets in the study.

Consent for publication
This section is not applicable since there are no details relating to individuals in the manuscript.

Competing interests
The authors declare no competing interests.

Author details
[1]Graduate Program in Veterinary Bioscience, Faculty of Veterinary Science, Chulalongkorn University, Bangkok, Thailand
[2]Veterinary Clinical Stem Cell and Bioengineering Research Unit, Faculty of Veterinary Science, Chulalongkorn University, Bangkok, Thailand
[3]Veterinary Stem Cell and Bioengineering Innovation Center (VSCBIC), Veterinary Pharmacology and Stem Cell Research Laboratory, Faculty of Veterinary Science, Chulalongkorn University, Bangkok, Thailand
[4]Department of Pharmacology, Faculty of Veterinary Science, Chulalongkorn University, Bangkok, Thailand
[5]Division of Veterinary Anatomy, Department of Veterinary Science, Faculty of Veterinary Medicine, Universitas Airlangga, Surabaya, Indonesia
[6]Immunology Research Center, Faculty of Dentistry, Chulalongkorn University, Bangkok, Thailand
[7]Center of Excellence in Periodontal Disease and Dental Implant, Chulalongkorn University, Bangkok, Thailand
[8]Center of Excellence for Dental Stem Cell Biology, Department of Anatomy, Faculty of Dentistry, Chulalongkorn University, Bangkok, Thailand
[9]Center of Excellence in Regenerative Dentistry, Faculty of Dentistry, Chulalongkorn University, Bangkok, Thailand
[10]Academic Affairs, Faculty of Veterinary Science, Chulalongkorn University, Bangkok, Thailand

Received: 14 June 2024 / Accepted: 26 August 2024
Published online: 09 September 2024

References

1. Vidal L, Kampleitner C, Brennan MA, Hoornaert A, Layrolle P. Reconstruction of large skeletal defects: current clinical therapeutic strategies and future directions using 3D printing. Front Bioeng Biotechnol. 2020;8:61.
2. Schmidt AH. Autologous bone graft: is it still the gold standard? Injury. 2021;52(Suppl 2):S18–22.
3. Campana V, Milano G, Pagano E, Barba M, Cicione C, Salonna G, et al. Bone substitutes in orthopaedic surgery: from basic science to clinical practice. J Mater Sci Mater Med. 2014;25(10):2445–61.
4. Wang W, Yeung KWK. Bone grafts and biomaterials substitutes for bone defect repair: a review. Bioact Mater. 2017;2(4):224–47.
5. Alonzo M, Primo FA, Kumar SA, Mudloff JA, Dominguez E, Fregoso G et al. Bone tissue engineering techniques, advances and scaffolds for treatment of bone defects. Curr Opin Biomed Eng. 2021;17.
6. Collins MN, Ren G, Young K, Pina S, Reis RL, Oliveira JM. Scaffold fabrication technologies and structure/function properties in bone tissue engineering. Adv Funct Mater. 2021;31(21).
7. Zhu L, Luo D, Liu Y. Effect of the nano/microscale structure of biomaterial scaffolds on bone regeneration. Int J Oral Sci. 2020;12(1):6.
8. Abbasi N, Hamlet S, Love RM, Nguyen N-T. Porous scaffolds for bone regeneration. J Science: Adv Mater Devices. 2020;5(1):1–9.
9. Flores-Jimenez MS, Garcia-Gonzalez A, Fuentes-Aguilar RQ. Review on porous scaffolds generation process: a tissue engineering approach. ACS Appl Bio Mater. 2023;6(1):1–23.
10. Dwivedi R, Kumar S, Pandey R, Mahajan A, Nandana D, Katti DS, et al. Polycaprolactone as biomaterial for bone scaffolds: review of literature. J Oral Biol Craniofac Res. 2020;10(1):381–8.
11. Cipitria A, Skelton A, Dargaville TR, Dalton PD, Hutmacher DW. Design, fabrication and characterization of PCL electrospun scaffolds—a review. J Mater Chem. 2011;21:26.
12. Mondal D, Griffith M, Venkatraman SS. Polycaprolactone-based biomaterials for tissue engineering and drug delivery: current scenario and challenges. Int J Polym Mater Polym Biomaterials. 2016;65(5):255–65.
13. Al-Sanabani JS, Madfa AA, Al-Sanabani FA. Application of calcium phosphate materials in dentistry. Int J Biomater. 2013;2013:876132.
14. Zhou H, Lee J. Nanoscale hydroxyapatite particles for bone tissue engineering. Acta Biomater. 2011;7(7):2769–81.
15. Ielo I, Calabrese G, De Luca G, Conoci S. Recent advances in hydroxyapatite-based biocomposites for bone tissue regeneration in orthopedics. Int J Mol Sci. 2022;23(17).
16. Dewi AH, Ana ID. The use of hydroxyapatite bone substitute grafting for alveolar ridge preservation, sinus augmentation, and periodontal bone defect: a systematic review. Heliyon. 2018;4(10):e00884.
17. Chuysinuan P, Nooeaid P, Thanyacharoen T, Techasakul S, Pavasant P, Kanjanamekanant K. Injectable eggshell-derived hydroxyapatite-incorporated fibroin-alginate composite hydrogel for bone tissue engineering. Int J Biol Macromol. 2021;193(Pt A):799–808.
18. Turnbull G, Clarke J, Picard F, Riches P, Jia L, Han F, et al. 3D bioactive composite scaffolds for bone tissue engineering. Bioact Mater. 2018;3(3):278–314.
19. Siri S, Wadbua P, Amornkitbamrung V, Kampa N, Maensiri S. Surface modification of electrospun PCL scaffolds by plasma treatment and addition of adhesive protein to promote fibroblast cell adhesion. Mater Sci Technol. 2010;26(11):1292–7.
20. Ebrahimi Z, Irani S, Ardeshirylajimi A, Seyedjafari E. Enhanced osteogenic differentiation of stem cells by 3D printed PCL scaffolds coated with collagen and hydroxyapatite. Sci Rep. 2022;12(1):12359.
21. Causa F, Netti PA, Ambrosio L, Ciapetti G, Baldini N, Pagani S, et al. Poly-epsilon-caprolactone/hydroxyapatite composites for bone regeneration: in vitro characterization and human osteoblast response. J Biomed Mater Res A. 2006;76(1):151–62.
22. Hajiali F, Tajbakhsh S, Shojaei A. Fabrication and properties of polycaprolactone composites containing calcium phosphate-based ceramics

and bioactive glasses in bone tissue engineering: a review. Polym Rev. 2017;58(1):164–207.
23. Rezania N, Asadi-Eydivand M, Abolfathi N, Bonakdar S, Mehrjoo M, Solati-Hashjin M. Three-dimensional printing of polycaprolactone/hydroxyapatite bone tissue engineering scaffolds mechanical properties and biological behavior. J Mater Sci Mater Med. 2022;33(3):31.
24. Cestari F, Petretta M, Yang Y, Motta A, Grigolo B, Sglavo VM. 3D printing of PCL/nano-hydroxyapatite scaffolds derived from biogenic sources for bone tissue engineering. Sustainable Mater Technol. 2021;29.
25. Hosseini FS, Soleimanifar F, Ardeshirylajimi A, Vakilian S, Mossahebi-Mohammadi M, Enderami SE, et al. In vitro osteogenic differentiation of stem cells with different sources on composite scaffold containing natural bioceramic and polycaprolactone. Artif Cells Nanomed Biotechnol. 2019;47(1):300–7.
26. Iaquinta MR, Mazzoni E, Bononi I, Rotondo JC, Mazziotta C, Montesi M, et al. Adult stem cells for bone regeneration and repair. Front Cell Dev Biol. 2019;7:268.
27. Mazzoni E, Mazziotta C, Iaquinta MR, Lanzillotti C, Fortini F, D'Agostino A, et al. Enhanced osteogenic differentiation of human bone marrow-derived mesenchymal stem cells by a hybrid hydroxylapatite/collagen scaffold. Front Cell Dev Biol. 2020;8:610570.
28. Nantavisai S, Pisitkun T, Osathanon T, Pavasant P, Kalpravidh C, Dhitavat S, et al. Systems biology analysis of osteogenic differentiation behavior by canine mesenchymal stem cells derived from bone marrow and dental pulp. Sci Rep. 2020;10(1):20703.
29. Chuenjitkuntaworn B, Osathanon T, Nowwarote N, Supaphol P, Pavasant P. The efficacy of polycaprolactone/hydroxyapatite scaffold in combination with mesenchymal stem cells for bone tissue engineering. J Biomed Mater Res A. 2016;104(1):264–71.
30. Wang T, Yang X, Qi X, Jiang C. Osteoinduction and proliferation of bone-marrow stromal cells in three-dimensional poly (epsilon-caprolactone)/hydroxyapatite/collagen scaffolds. J Transl Med. 2015;13:152.
31. Granchi D, Ochoa G, Leonardi E, Devescovi V, Baglio SR, Osaba L, et al. Gene expression patterns related to osteogenic differentiation of bone marrow-derived mesenchymal stem cells during ex vivo expansion. Tissue Eng Part C Methods. 2010;16(3):511–24.
32. Nantavisai S, Egusa H, Osathanon T, Sawangmake C. Mesenchymal stem cell-based bone tissue engineering for veterinary practice. Heliyon. 2019;5(11):e02808.
33. Ward E. A review of tissue engineering for periodontal tissue regeneration. J Vet Dent. 2022;39(1):49–62.
34. Alves EG, Serakides R, Boeloni JN, Rosado IR, Ocarino NM, Oliveira HP, et al. Comparison of the osteogenic potential of mesenchymal stem cells from the bone marrow and adipose tissue of young dogs. BMC Vet Res. 2014;10:190.
35. Huang J, Tian B, Chu F, Yang C, Zhao J, Jiang X, et al. Rapid maxillary expansion in alveolar cleft repaired with a tissue-engineered bone in a canine model. J Mech Behav Biomed Mater. 2015;48:86–99.
36. Dominici M, Le Blanc K, Mueller I, Slaper-Cortenbach I, Marini F, Krause D, et al. Minimal criteria for defining multipotent mesenchymal stromal cells. The International Society for Cellular Therapy position statement. Cytotherapy. 2006;8(4):315–7.
37. Teunissen M, Verseijden F, Riemers FM, van Osch G, Tryfonidou MA. The lower in vitro chondrogenic potential of canine adipose tissue-derived mesenchymal stromal cells (MSC) compared to bone marrow-derived MSC is not improved by BMP-2 or BMP-6. Vet J. 2021;269:105605.
38. Dang Le Q, Rodprasert W, Kuncorojakti S, Pavasant P, Osathanon T, Sawangmake C. In vitro generation of transplantable insulin-producing cells from canine adipose-derived mesenchymal stem cells. Sci Rep. 2022;12(1):9127.
39. Wang W, Yuan C, Liu Z, Geng T, Li X, Wei L, et al. Characteristic comparison between canine and human dental mesenchymal stem cells for periodontal regeneration research in preclinical animal studies. Tissue Cell. 2020;67:101405.
40. Boxall SA, Jones E. Markers for characterization of bone marrow multipotential stromal cells. Stem Cells Int. 2012;2012:975871.
41. Brennan MA, Renaud A, Gamblin AL, D'Arros C, Nedellec S, Trichet V, et al. 3D cell culture and osteogenic differentiation of human bone marrow stromal cells plated onto jet-sprayed or electrospun micro-fiber scaffolds. Biomed Mater. 2015;10(4):045019.
42. Declercq HA, Desmet T, Dubruel P, Cornelissen MJ. The role of scaffold architecture and composition on the bone formation by adipose-derived stem cells. Tissue Eng Part A. 2014;20(1–2):434–44.
43. Li S, Tallia F, Mohammed AA, Stevens MM, Jones JR. Scaffold channel size influences stem cell differentiation pathway in 3-D printed silica hybrid scaffolds for cartilage regeneration. Biomater Sci. 2020;8(16):4458–66.
44. Lu X, Wang Y, Jin F. Influence of a non-biodegradable porous structure on bone repair. RSC Adv. 2016;6(84):80522–8.
45. Murugan S, Parcha SR. Fabrication techniques involved in developing the composite scaffolds PCL/HA nanoparticles for bone tissue engineering applications. J Mater Sci Mater Med. 2021;32(8):93.
46. Ghasemi M, Turnbull T, Sebastian S, Kempson I. The MTT assay: utility, limitations, pitfalls, and interpretation in bulk and single-cell analysis. Int J Mol Sci. 2021;22(23).
47. Malda J, Klein TJ, Upton Z. The roles of hypoxia in the in vitro engineering of tissues. Tissue Eng. 2007;13(9):2153–62.
48. Totaro A, Salerno A, Imparato G, Domingo C, Urciuolo F, Netti PA. PCL-HA microscaffolds for in vitro modular bone tissue engineering. J Tissue Eng Regen Med. 2017;11(6):1865–75.
49. Xu J, Li Z, Hou Y, Fang W. Potential mechanisms underlying the Runx2 induced osteogenesis of bone marrow mesenchymal stem cells. Am J Transl Res. 2015;7(12):2527–35.
50. Chan WCW, Tan Z, To MKT, Chan D. Regulation and role of transcription factors in osteogenesis. Int J Mol Sci. 2021;22(11).
51. Huang W, Yang S, Shao J, Li YP. Signaling and transcriptional regulation in osteoblast commitment and differentiation. Front Biosci. 2007;12:3068–92.
52. Erickson CB, Payne KA. Inductive signals and progenitor fates during osteogenesis. Reference Module in Biomedical Sciences. 2018.
53. Amarasekara DS, Kim S, Rho J. Regulation of osteoblast differentiation by cytokine networks. Int J Mol Sci. 2021;22(6).
54. Salari Sedigh H, Saffarpour A, Jamshidi S, Ashouri M, Nassiri SM, Dehghan MM, et al. In vitro investigation of canine periodontal ligament-derived mesenchymal stem cells: a possibility of promising tool for periodontal regeneration. J Oral Biol Craniofac Res. 2023;13(3):403–11.
55. Holm E, Gleberzon JS, Liao Y, Sorensen ES, Beier F, Hunter GK, et al. Osteopontin mediates mineralization and not osteogenic cell development in vitro. Biochem J. 2014;464(3):355–64.
56. Sawangmake C, Nantavisai S, Osathanon T, Pavasant P. Osteogenic differentiation potential of canine bone marrow-derived mesenchymal stem cells under different β-glycerophosphate concentrations in vitro. Thai J Veterinary Med. 2016;46(4):617–25.
57. Rodprasert W, Nantavisai S, Pathanachai K, Pavasant P, Osathanon T, Sawangmake C. Tailored generation of insulin producing cells from canine mesenchymal stem cells derived from bone marrow and adipose tissue. Sci Rep. 2021;11(1):12409.
58. Thadavirul N, Pavasant P, Supaphol P. Improvement of dual-leached polycaprolactone porous scaffolds by incorporating with hydroxyapatite for bone tissue regeneration. J Biomater Sci Polym Ed. 2014;25(17):1986–2008.
59. Purbantoro SD, Osathanon T, Nantavisai S, Sawangmake C. Osteogenic growth peptide enhances osteogenic differentiation of human periodontal ligament stem cells. Heliyon. 2022;8(7):e09936.

Publisher's note